Journal of Engineering Physics and Thermophysics, Vol. 81, No. 4, 2008

THE EFFECTS OF MHD ON FREE-CONVECTION FLOW PAST A SEMI-INFINITE ISOTHERMAL INCLINED PLATE

G. Palani and Kwang-Yong Kim

UDC 536.25

An analysis of the effects of MHD on a two-dimensional free-convective flow of a viscous incompressible fluid past a semi-infinite isothermal inclined plate is carried out. The effects of viscous dissipation and the induced magnetic field are assumed to be negligible. A more accurate, unconditionally stable, and fast converging implicit finite difference scheme is used to solve the dimensionless governing equations. The effects of MHD on velocity, temperature, local and average skin friction, and local and average Nusselt number are studied. It is observed that the magnetic field parameter has a retarding effect on the velocity.

Introduction. The study of flow problems involving heat transfer is of primary importance in the fields of modern engineering design and operation of various kinds of machinery. Buoyancy-driven flows are of common occurrence in technological, atmospheric, and oceanic phenomena, with the buoyancy stratification being achieved often by the temperature field.

Due to its numerous applications, the study of the natural convection heat transfer from the differently-inclined surfaces has received much attention in recent years, both theoretically and experimentally. A lot of detailed studies have been made on the problem of natural convection on a vertical plate. At the same time, very little attention has been given to the problem of natural convection over inclined and horizontal plates or the plates slightly inclined to the horizontal. However, free-convection heat transfer from an inclined surface is very frequently encountered in engineering devices and natural environment. The unsteady natural convection flow past a semi-infinite vertical plate was first considered by Hellums and Churchill [1] with the use of an explicit finite difference scheme. This scheme suffers from some deficiencies, and hence a more efficient implicit finite difference scheme was used by Soundalgekar and Ganesan [2]. During last few years, attention was given to natural convection flows past inclined plates.

Kierkus [3] presented a perturbation analysis for a two-dimensional laminar free-convection flow about an inclined isothermal plate in air and studied the problem experimentally for different angles of inclination. Pera and Gebhart [4] studied the laminar natural convection boundary-layer flow above horizontal and inclined surfaces with uniform temperatures and heat fluxes. Chen et al. [5] obtained a numerical solution for the problem of natural convection over an inclined plate with a variable surface temperature. Ganesan and Ekambavannan [6] solved the problem of transient free-convective flow of an incompressible viscous fluid past a semi-infinite isothermal plate by an implicit finite difference method which is unconditionally stable. Callahan and Marner [7] gave a numerical solution for free convection with mass transfer on an isothermal vertical flat plate by employing an explicit finite difference scheme.

The problem of free convection of an electrically conducting fluid past a plate under the influence of a magnetic field is important for gaining an understanding of such flows and for possible application in geophysics, astrophysics, and aerodynamics. An exact analysis of the MHD Stokes problem for the flow of an electrically conducting, incompressible viscous fluid past an impulsively started vertical plate under the action of transversely applied magnetic field was carried out by Soundalgekar et al. [8]. Sacheti et al. [9] obtained an exact solution for unsteady magnetohydrodynamic free-convection flow on an impulsively started vertical plate with a constant heat flux. Elbashbeshy [10] studied heat and mass transfer along a vertical plate under combined buoyancy effects of thermal and species diffusion in the presence of magnetic field. Ganesan and Palani [11] considered the effects of MHD on a two-dimensional free-convective flow of a viscous incompressible fluid past a semi-infinite isothermal vertical plate using an efficient im-

Department of Mechanical Engineering, Inha University, Incheon 402-751, Republic of Korea; email: gpalani32@yahoo.co.in. Published in Inzhenerno-Fizicheskii Zhurnal, Vol. 81, No. 4, pp. 697–704, July–August, 2008. Original article submitted April 2, 2007; revision submitted November 12, 2007.

plicit finite difference method. Here, the dimensionless governing equations are unsteady, two-dimensional, coupled, nonlinear integro-differential equations which are solved numerically using an implicit finite difference scheme.

In recent years, the effects of the transverse magnetic field on the flow of an incompressible, viscous, electrically conducting fluid have also been studied extensively by many researchers. However, unsteady natural convection MHD flows past a semi-infinite isothermal inclined plate has not received any attention in the literature. Hence, we propose to consider this problem.

Governing Equations and Boundary Conditions. Transient free-convective laminar flow of an incompressible viscous fluid past a semi-infinite isothermal inclined plate under the action of magnetic field is considered. It is assumed that initially, at time $t' \le 0$, the plate and the fluid are at the same temperature and at $t' > 0$ the temperature of the plate is suddenly raised to T'_{w}, causing the flow in its vicinity. The x and y axes are measured along the plate and the upward normal to it, respectively. The plate is inclined at an angle ϕ to the horizontal. The effect of viscous dissipation is neglected in the energy equation. A uniform transverse magnetic field is applied along the y axis. It is also assumed that the induced magnetic field is negligible. Then, under these assumptions, the governing boundary-layer equations of mass, momentum, and energy for free-convection flows with the Boussinesq approximation are as follows:

$$\frac{\partial u}{\partial x} + \frac{\partial v}{\partial y} = 0 , \tag{1}$$

$$\frac{\partial u}{\partial t'} + u\frac{\partial u}{\partial x} + v\frac{\partial u}{\partial y} = g\beta\cos\phi\frac{\partial}{\partial x}\int_y^\infty (T' - T'_\infty)\,dy + g\beta\sin\phi\,(T' - T'_\infty) + \nu\frac{\partial^2 u}{\partial y^2} - \frac{\sigma B_0^2}{\rho}u , \tag{2}$$

$$\frac{\partial T'}{\partial t'} + u\frac{\partial T'}{\partial x} + v\frac{\partial T'}{\partial y} = \alpha\frac{\partial^2 T'}{\partial y^2} . \tag{3}$$

The initial and boundary conditions are

$$t' \le 0: \quad u = 0 , \quad v = 0 , \quad T' = T'_\infty ;$$

$$t' > 0: \quad u = 0 , \quad v = 0 , \quad T' = T'_{\mathrm{w}} \quad \text{at} \quad y = 0 ,$$

$$u = 0 , \quad T' = T'_\infty \quad \text{at} \quad x = 0 ,$$

$$u \to 0 , \quad T' \to T'_\infty \quad \text{as} \quad y \to \infty . \tag{4}$$

The local and average skin friction are given respectively as

$$\tau_x = \mu\left(\frac{\partial u}{\partial y}\right)_{y=0} , \tag{5}$$

$$\bar{\tau}_L = \frac{1}{L}\int_0^L \mu\left(\frac{\partial u}{\partial y}\right)_{y=0} dx . \tag{6}$$

The local and average Nusselt numbers are equal respectively to

$$\mathrm{Nu}_x = \frac{-x\left(\dfrac{\partial T'}{\partial y}\right)_{y=0}}{T'_{\mathrm{w}} - T'_{\infty}}, \tag{7}$$

$$\overline{\mathrm{Nu}}_L = -\int_0^L \frac{\left(\dfrac{\partial T'}{\partial y}\right)_{y=0}}{T'_{\mathrm{w}} - T'_{\infty}}\, dx\,. \tag{8}$$

We introduce the following dimensionless quantities:

$$X = \frac{x}{L},\quad Y = \frac{y}{L}\mathrm{Gr}^{1/4},\quad U = \frac{uL}{\nu}\mathrm{Gr}^{-1/2},\quad V = \frac{vL}{\nu}\mathrm{Gr}^{-1/4},\quad t = \frac{\nu t'}{L^2}\mathrm{Gr}^{1/2},\quad T = \frac{T' - T'_{\infty}}{T'_{\mathrm{w}} - T'_{\infty}},$$

$$\mathrm{Gr} = \frac{g\beta L^3 (T'_{\mathrm{w}} - T'_{\infty})}{\nu^2},\quad \mathrm{M} = \frac{\sigma B_0^2 L^2}{\rho\nu}\mathrm{Gr}^{-1/2},\quad \mathrm{Pr} = \frac{\nu}{\alpha}. \tag{9}$$

Then Eqs. (1)—(3) are reduced to the dimensionless form

$$\frac{\partial U}{\partial X} + \frac{\partial V}{\partial Y} = 0, \tag{10}$$

$$\frac{\partial U}{\partial t} + U\frac{\partial U}{\partial X} + V\frac{\partial U}{\partial Y} = \mathrm{Gr}^{-1/4}\cos\phi\,\frac{\partial}{\partial X}\int_Y^{\infty} T dY + T\sin\phi + \frac{\partial^2 U}{\partial Y^2} - \mathrm{M}U, \tag{11}$$

$$\frac{\partial T}{\partial t} + U\frac{\partial T}{\partial X} + V\frac{\partial T}{\partial Y} = \frac{1}{\mathrm{Pr}}\frac{\partial^2 T}{\partial Y^2}. \tag{12}$$

The corresponding initial and boundary conditions for dimensionless quantities are given as

$$t \le 0:\ \ U = 0,\ \ V = 0,\ \ T = 0;$$

$$t > 0:\ \ U = 0,\ \ V = 0,\ \ T = 1 \quad \text{at}\ \ Y = 0,$$

$$U = 0,\ \ T = 0 \quad \text{at}\ \ X = 0,$$

$$U \to 0,\ \ T \to 0 \quad \text{as}\ \ Y \to \infty. \tag{13}$$

The expressions for the dimensionless local and average skin friction and the relations for the Nusselt number are

$$\tau_X = \mathrm{Gr}^{3/4}\left(\frac{\partial U}{\partial Y}\right)_{Y=0}, \tag{14}$$

$$\bar{\tau} = \mathrm{Gr}^{3/4} \int_0^1 \left[\frac{\partial U}{\partial Y}\right]_{Y=0} dX\,, \tag{15}$$

$$\mathrm{Nu}_X = -X\,\mathrm{Gr}^{1/4} \left(\frac{\partial T}{\partial Y}\right)_{Y=0}\,, \tag{16}$$

$$\overline{\mathrm{Nu}} = -\,\mathrm{Gr}^{1/4} \int_0^1 \left(\frac{\partial T}{\partial Y}\right)_{Y=0} dX\,. \tag{17}$$

Finite Difference Method. The two-dimensional, nonlinear, unsteady, coupled integro-differential equations (10)—(12) under the initial and boundary conditions (13) are solved using an implicit finite difference scheme of Crank—Nicolson type which is rapidly convergent and unconditionally stable. The finite difference equations corresponding to Eqs. (10)—(12) are given as

$$\frac{U_{i,j-1}^{k+1} - U_{i-1,j-1}^{k+1} + U_{i,j}^{k+1} - U_{i-1,j}^{k+1} + U_{i,j-1}^{k} - U_{i-1,j-1}^{k} + U_{i,j}^{k} - U_{i-1,j}^{k}}{4\Delta X} + \frac{V_{i,j}^{k+1} - V_{i,j-1}^{k+1} + V_{i,j}^{k} - V_{i,j-1}^{k}}{2\Delta Y} = 0\,, \tag{18}$$

$$\frac{U_{i,j}^{k+1} - U_{i,j}^{k}}{\Delta t} + U_{i,j}^{k} \frac{U_{i,j}^{k+1} - U_{i-1,j}^{k+1} + U_{i,j}^{k} - U_{i-1,j}^{k}}{2\Delta X} + V_{i,j}^{k} \frac{U_{i,j+1}^{k+1} - U_{i,j-1}^{k+1} + U_{i,j+1}^{k} - U_{i,j-1}^{k}}{4\Delta Y}$$

$$= \mathrm{Gr}^{-1/4} \cos\phi \frac{\partial}{\partial X} \int_Y^{\infty} T dY + \sin\phi \frac{T_{i,j}^{k+1} + T_{i,j}^{k}}{2}$$

$$+ \frac{U_{i,j-1}^{k+1} - 2U_{i,j}^{k+1} + U_{i,j+1}^{k+1} + U_{i,j-1}^{k} - 2U_{i,j}^{k} + U_{i,j+1}^{k}}{2\Delta Y^2} - \mathrm{M} \frac{U_{i,j}^{k+1} + U_{i,j}^{k}}{2}\,, \tag{19}$$

$$\frac{T_{i,j}^{k+1} - T_{i,j}^{k}}{\Delta t} + U_{i,j}^{k} \frac{T_{i,j}^{k+1} - T_{i-1,j}^{k+1} + T_{i,j}^{k} - T_{i-1,j}^{k}}{2\Delta X} + V_{i,j}^{k} \frac{T_{i,j+1}^{k+1} - T_{i,j-1}^{k+1} + T_{i,j+1}^{k} - T_{i,j-1}^{k}}{4\Delta Y}$$

$$= \frac{T_{i,j-1}^{k+1} - 2T_{i,j}^{k+1} + T_{i,j+1}^{k+1} + T_{i,j-1}^{k} - 2T_{i,j}^{k} + T_{i,j+1}^{k}}{2\mathrm{Pr}\,(\Delta Y)^2}\,. \tag{20}$$

The values of U, V, and T are known at all grid points at $t = 0$ from the initial conditions. During any time step, $U_{i,j}^{k}$ and $V_{i,j}^{k}$ appearing in the finite difference equation are treated as constants. The values of U, V, and T are calculated at the $(k+1)$th time level using the known values at the previous kth time level in the following way. Equation (20) at every internal nodal point for a particular value of i constitutes a tridiagonal system of equations which are solved by the Thomas algorithm described by Carnahan et al. [12]. Thus, the values of T are found at every nodal point at the $(k+1)$th time level. On the basis of these values, the values of U at the $(k+1)$th time level are obtained from Eq. (19) in a similar manner. The integrals in this equation are evaluated by the Newton—Cotes closed integration formula. Then the values of V are calculated explicitly from Eq. (18) at every nodal point on a particular ith level. This process is repeated for all values of i. Thus, the values of T, U, and V are known at all grid points in the rectangular region at the $(k+1)$th time level.

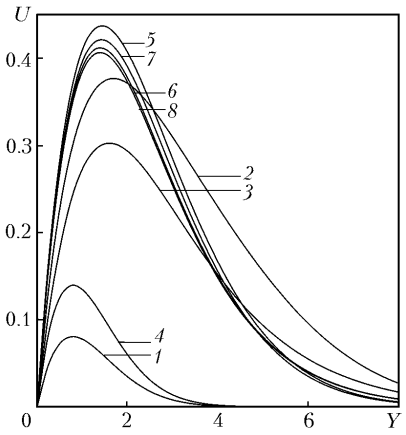

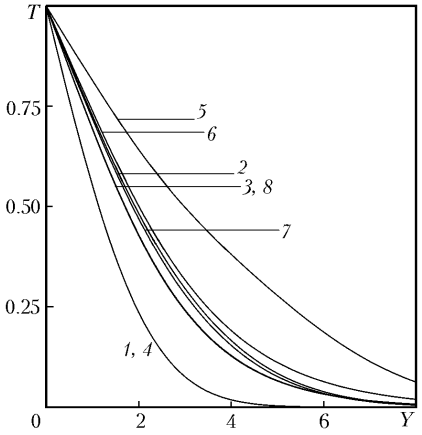

Fig. 1. Transient and steady-state velocity profiles at X = 1, Pr = 0.7, M = 0.5, and different values of ϕ, Gr, and t: 1) $\phi = 30^o$, $Gr = 10^6$, and t = 0.75; 2) 30^o, 10^6, and 4.23; 3) 30^o, 10^6, and 7.03*; 4) 60^o, 10^5, and 0.75; 5) 60^o, 10^5, and 3.18; 6) 60, 10^5, and 5.75*; 7) 60^o, 10^6, and 3.20; 8) 60^o, 10^6, and 5.82*. Hereinafter, the asterisk corresponds to a steady state.

Fig. 2. Transient and steady-state temperature profiles at X = 1, Pr = 0.7, M = 0.5, and different values of ϕ, Gr, and t: 1) $\phi = 30^o$, $Gr = 10^5$, and t = 1; 2) 30^o, 10^5, and 2.95; 3) 30^o, 10^5, and 5.75*; 4) 30^o, 10^6, and 1; 5) 30^o, 10^6, and 4.07; 6) 30^o, 10^6, and 7.03*; 7) 60^o, 10^6, and 2.91; 8) 60^o, 10^6, and 5.82*.

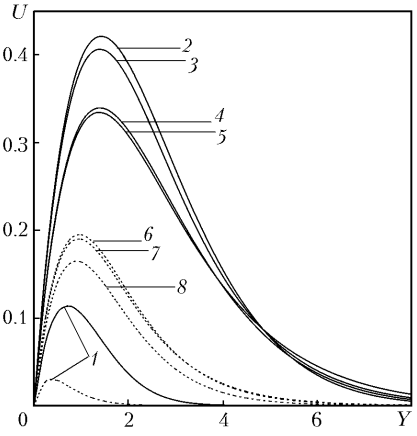

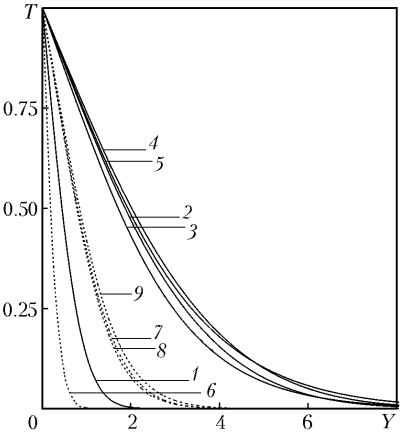

Fig. 3. Transient and steady-state velocity profiles at X = 1, $Gr = 10^6$, ϕ for different values of Pr, M, and t: 1) M = 0.5 and t = 0.6; 2) 0.5 and 3.2; 3) 0.5 and 5.82*; 4) 1 and 3.66; 5) 1 and 6.93*; 6) 0.5 and 5.64; 7) 0.5 and 7.18*; 8) 1 and 7.63*. Solid and dotted curves correspond to Pr = 0.7 and 7, respectively.

Fig. 4. Transient and steady-state temperature profiles at X = 1, $Gr = 10^6$, $\phi = 60^o$ for different values of Pr, M, and t: 1) M = 0.5 and t = 0.15; 2) 0.5 and 2.94; 3) 0.5 and 5.82*; 4) 1 and 3.39; 5) 1 and 6.93*; 6) 0.5 and 0.25; 7) 0.5 and 5.62; 8) 0.5 and 7.18*; 9) 1 and 7.63*.

This process is repeated in time until a steady state is reached, which is assumed to take place when the absolute differences between the values of U, as well as of the temperature T, at two consecutive time steps are less than 10^{-5} for all grid points. Computations have been carried out for different values of parameters.

The derivatives involved in Eqs. (14)—(17) are evaluated using a five-point approximation formula and then the integrals are calculated using the Newton-Cotes closed integration formula.

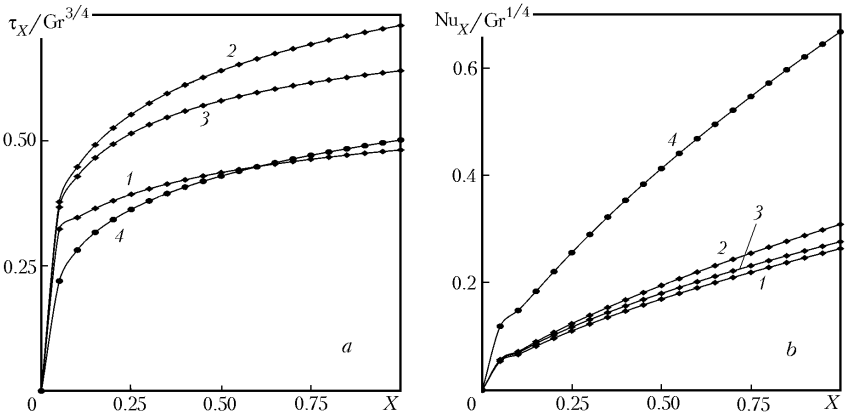

Fig. 5. Local skin friction (a) and Nusselt number (b) as functions of longitudinal coordinate X at Gr = 10^6: 1) Pr = 0.7, M = 0.5, and $\phi = 30^o$; 2) 0.7, 0.5, and 60^o; 3) 0.7, 1, and 60^o; 4) 7, 0.5, and 60^o.

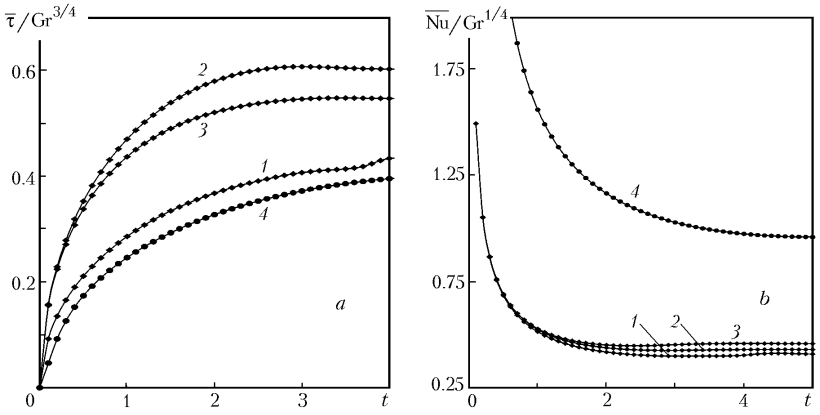

Fig. 6. Average skin friction (a) and Nusselt number (b) as time functions. The notation of the curves is same as in Fig. 5.

The region of integration is considered as a rectangle with the sides $X_{\max} = 1.0$ and $Y_{\max} = 16.0$, where $Y_{\max}$ corresponding to infinity lies far outside the momentum and thermal boundary layers. After experimenting with a few sets of mesh sizes, they are fixed as $\Delta X = 0.05$, $\Delta Y = 0.25$, and $\Delta t = 0.01$. The Crank—Nicolson implicit finite difference scheme is always stable and convergent.

Results and Discussion. Transient velocity and temperature profiles for different values of Gr and ϕ are shown in Figs. 1 and 2, respectively. Temporal maximum in these profiles can be seen. This type of phenomenon was observed by several investigators for the problem of transient free convection on a vertical and an inclined plate. When ϕ increases, the normal component of the buoyancy force decreases near the leading edge, which causes an impulsive driving force for fluid motion along the plate. That is, the impulsive force along the plate decreases with increasing ϕ. Due to these facts, the difference between the temporal maximum and steady-state values decreases. The time taken to reach a steady state decreases with increase in ϕ. Since the tangential buoyancy force dominates downstream and increases with ϕ, the velocity also increases but the reverse situation is observed in the case of temperature distribution. It is seen that the velocity decreases but the temperature increases with increasing value of the Grashof number. From the numerical results we observe that there is no appreciable change in the temperature distribution due to the change in the Grashof number at the initial period of time. It is also evident that the time taken to reach a steady state is larger for higher values of Gr. The difference between the temporal maximum and steady-state values is reduced with an increasing Gr.

Figures 3 and 4 show the effect of the Prandtl number and the magnetic field parameter on the transient velocity and temperature distributions at the upper edge of the plate, viz. at $X = 1$. Both velocity and temperature de-

crease as Pr increases. It is observed that the time taken to reach the steady state increases with Pr and M. We observe from Fig. 3 that the magnetic field parameter M has a retarding effect on velocity but, as is seen in Fig. 4, the reverse regularity takes place for the temperature distribution. The difference between the temporal maximum and steady-state values decreases with an increasing M. No temporal maximum is observed for higher values of M.

The local skin friction is shown in Fig. 5a. The local wall shear stress decreases as M increases or ϕ decreases. This occurs because of the fact that the velocity gradient decreases near the plate as M increases or ϕ decreases, which is seen in Fig. 1. It is also observed that the local wall shear stress is larger for lower Prandtl number.

The steady-state local Nusselt number is shown in Fig. 5b. It is seen that it increases with X. The local heat transfer depends more strongly on Pr than on other parameters, since a lower Pr gives thicker temperature profiles, which agrees with Fig. 4. Large values of Nusselt number are observed for higher Pr. The Nusselt number decreases as M increases. It is also observed that the local Nusselt number increases with the inclination angle ϕ.

The average values of skin friction and Nusselt numbers are shown in Fig. 6. The average skin friction decreases as the inclination angle ϕ diminishes. This is due to the fact that the tangential component of buoyancy force that directly contributes to the motion in the streamwise direction decreases with ϕ. The average skin friction decreases with increasing M. It is also observed that this friction for air is greater than for water irrespective of other parameters of the problem. It should be noted that for short times the average Nusselt number is constant for various values of the parameters considered. This shows that initially there is only heat conduction. Then the average Nusselt number begins to decrease with increasing value of M. It increases with ϕ. A higher value of Nusselt number is observed for a larger value of Pr.

CONCLUSIONS

1. The magnetic field parameter M has a retarding effect on the velocity.
2. No temporal maximum is observed for higher value of M.
3. The velocity increases with ϕ throughout the transient period and in a steady state.
4. The difference between the temporal maximum and steady-state values decreases with an increasing ϕ.
5. The local and average Nusselt numbers increase with Pr.
6. The increase in the magnetic field parameter reduces the average Nusselt number.

NOTATION

B_0, magnetic field strength; Gr, Grashof number; g, acceleration due to gravity; L, reference length; M, magnetic parameter; Nu_x, Nu_X, local Nusselt numbers; $\overline{\mathrm{N}}\ \mu$, $\overline{\mathrm{Nu}}$, average Nusselt numbers; Pr, Prandtl number; T', temperature; T, dimensionless temperature; t', time; T, dimensionless time; u and v, velocity components in x and y directions, respectively; U and V, dimensionless velocity components in X and Y directions; x and y, spatial coordinates along the plate and upward normal to it; X and Y, dimensionless spatial coordinates; α, thermal diffusivity; β, volumetric coefficient of thermal expansion; ϕ, angle of inclination of the plate to horizontal; μ, dynamic viscosity; ν, kinematic viscosity; ρ, density; σ, electrical conductivity of the fluid; τ_x, local skin friction; τ_X, dimensionless local skin friction; $\bar{\tau}_L$, average skin friction; $\bar{\tau}$, dimensionless average skin friction. Subscripts and superscripts: i and j, grid points along X and Y directions; k, time step level; max, maximum; w, on the wall; ∞, free stream conditions.

REFERENCES

1. J. D. Hellums and S. W. Churchill, Transient and steady state, free and natural convection, numerical solutions. Part 1. The isothermal vertical plate, *AIChE J.,* **8**, 90—92 (1962).
2. V. M. Soundalgekar and P. Ganesan, Finite difference analysis of transient free convection on an isothermal vertical flat plate, *Regional J., Energy Heat Mass Transfer*, **13**, 219—224 (1981).
3. W. T. Kierkus, An analysis of laminar free convection flow and heat transfer about an inclined isothermal plate, *Int. J. Heat Mass Transfer*, **11**, 241—253 (1968).

4. L. Pera and B. Gebhart, Natural convection boundary layer flow over horizontal and slightly inclined surfaces, *Int. J. Heat Mass Transfer*, **16**, 1131—1146 (1973).
5. T. S. Chen, H. C. Tien, and B. F. Armaly, Natural convection on horizontal, inclined and vertical plates with variable surface temperature or heat flux, *Int. J. Heat Mass Transfer*, **29**, 1465—1478 (1986).
6. P. Ganesan and K. Ekambavannan, Numerical solution of unsteady natural convection on isothermal inclined plate, *Indian J. of Technol.*, **30**, 471—476 (1992).
7. G. D. Callahan and W. J. Marner, Transient free convection with mass transfer on an isothermal vertical flat plate, *Int. J. Heat Mass Transfer,* **19**, 165—174 (1976).
8. V. M. Soundalgekar, S. K. Gupta, and R. N. Arnake, Free convection effects on MHD Stokes problem for a vertical plate, *Nucl. Eng. Des.*, **51**, 403-407 (1979).
9. Nirmal C. Sacheti, Pallath Chandran, and A. K. Singh, An exact solution for unsteady magnetohydrodynamic free convection flow with constant heat flux, *Int. Commun. Heat Mass Transfer*, **21**, 131—142 (1994).
10. E. M. A. Elbashbeshy, Heat and mass transfer along a vertical plate with variable surface tension and concentration in the presence of the magnetic field, *Int. J. Eng. Sci.*, **34**, No. 5, 515—522 (1997).
11. P. Ganesan and G. Palani, Numerical solution of unsteady MHD flow past semi-infinite isothermal vertical plate, *Proc. 17th National & 6th ISHMT/ASME Heat & Mass Transfer Conf.*, Kalpakkam, India (2004), pp. 184—188.
12. B. Carnahan, H. A. Luther, and J. O. Wilkes, *Applied Numerical Methods*, John Wiley and Sons, New York (1969).